ELSEVIER

Ceramics International 26 (2000) 849–854

CERAMICS INTERNATIONAL

Potential of SiC as a heat exchanger material in combined cycle plant

Marc Steen [a,*], Luigi Ranzani [b]

[a] *Institute for Advanced Materials, Joint Research Centre, European Commission, PO Box 2, NL-1755 ZG Petten, The Netherlands*
[b] *ENEL Research, Via Volta 1, 20093 Cologno Monzese (MI), Italy*

Received 24 September 1999; received in revised form 10 January 2000; accepted 8 February 2000

Abstract

The short and long term mechanical properties of a sintered silicon carbide intended as a heat exchanger material have been investigated. The short term strength shows an acceptable scatter characterised by a Weibull modulus of seven from room temperature up to 1400°C. In the time-dependent regime failure occurs by subcritical crack growth from surface located inherent defects at high stresses. Below a threshold stress oxidation blunting of these surface defects occurs and causes a transition from subritical crack growth to diffusion creep as life-limiting mechanism. Unlike other ceramics, the threshold stress for subcritical crack growth falls within the low probability range of fast fracture. Failure mechanism maps presenting the life-limiting mechanisms of the investigated sintered silicon carbide over a range of stresses and temperatures are presented.

Keywords: D. SiC; E. Heat exchanger; Combined cycle plant

1. Introduction

Future improved coal-fired power stations must have a minimal environmental impact, and operate at much higher thermal efficiencies than the present systems. They must have low emission of NO_x, SO_x and particulates, and will have lower CO_2 emissions due to a higher thermal efficiency of the overall power generation cycle. Large efficiency improvements require a change to gas turbines (Brayton cycle) instead of exclusive reliance on steam turbines (Rankine cycle). In order to increase the efficiency of the gas turbine, the turbine working fluid should be at the highest possible temperature. To avoid corrosion and erosion problems in turbine components such as stators and rotors, the working fluid must be clean and not contain coal ash, which can be achieved by using air instead of combustion gas. This approach requires the use of a ceramic heat exchanger to separate the coal combustion product stream from the turbine inlet air.

The leading materials for high temperature pressurised heat exchanger application are silicon carbide based ceramics due to their relatively low cost and demonstrated fabrication technology relative to alternate refractory materials. Much improvement in the properties of these materials has been achieved to the point that they are reaching a maturity as engineering materials. Short term high temperature property data for clean environments are available. However, the amount of long term data for creep and subcritical crack growth, the main lifetime governing mechanisms at high temperatures, is limited. This paper presents the results of an investigation into the long-term mechanical behaviour of a commercially available sintered alpha-silicon carbide at temperatures relevant for service as a heat exchanger material in advanced gas turbine containing coal-fired power plants.

2. Material and testing procedure

The material used in this investigation is a sintered alpha-silicon carbide (Carborundum, USA). Some properties as supplied by the manufacturer are listed in Table 1. The material was received in the form of ready made tensile and bend specimens which had been taken out of a single batch of tubes and machined to the same surface finish.

* Corresponding author. Tel.: +31-224-565271; fax: +31-224-532036.
E-mail address: steen@jrc.nl (M. Steen).

0272-8842/00/$20.00
PII: S0272-8842(00)00027-4

Table 1
Material properties according to the manufacturer

Sintering aid	$\leqslant$ 0.4% B
Average grain size	3 to 6 micrometer
Second phase content	Trace impurities
Density	3.1 g/cm^3
Porosity	Negligible
Elastic modulus at room temperature	410 GPa
Poisson ratio	0.14
Four-point bend strength at room temperature	379 MPa
Weibull modulus	7
Hardness	2800 (Knoop)

The flexural test specimens have been prepared and tested according to the European standards EN 843-1 and EN 820-1 (strength testing resp. at room and elevated temperatures) and EN 820-4 (flexural creep testing). In the absence of a European standard for uniaxial strength and creep testing of monolithic ceramics, the ASTM standards C1273 (strength at room temperature) and C1291 (creep at high temperature) have been followed where possible and appropriate for uniaxial strength and creep tests.

3. Strength properties

The short-term strength has been determined by flexural tests in air at temperatures of 1250 and 1400°C. The average flexural strength±one standard deviation is shown as a function of temperature in Fig. 1, where data from literature [1–4] also included. Comparison with the literature data is only possible in qualitative terms because the effective volumes in the test pieces used in different literature studies may be different from that in this investigation. Nevertheless, the data show that the strength of sintered SiC only weakly depends on temperature up to 1400°C. Within the statistical scatter a constant Weibull modulus of 7 is observed for the investigated material from room temperature up to 1400°C, indicating that the same flaw population is limiting the strength at all temperatures.

4. Long term flexural properties

The long term high temperature properties have been investigated by constant load tests in air at 1250 and 1400°C under flexural loading and at 1400°C under uniaxial tensile loading. The strain evolution with time in the flexure tests exhibits primary and extended secondary creep stages, indicating that the outer fibre stress does not change with time and hence that a stationary stress distribution is reached in the flexural constant load tests. Tertiary creep has only been observed in one test at 1250°C. In all cases the strain to failure is very low, typically around 0.1%. After re-assembly none of the failed test specimens exhibits a permanent deflection.

The rupture lives at 1250 and 1400°C are plotted versus the applied flexural stress in Fig. 2. A large scatter, amounting to three orders of magnitude in life at a given stress level is observed at both temperatures, and the stress exponent for SCG determined from linear regression analysis ranges from 22.6 at 1250°C to 13.7 at 1400°C. These high values indicate that subcritical crack growth from inherent defects is the life-limiting factor under constant load, and are at the same time sufficiently low to take the time-dependence of strength into account for design purposes. Also, at both temperatures, the strength data can be fitted to the regression line of the constant load data. The same observations can be made for the minimum strain rate as a function of stress, although the scatter there amounts to two orders of magnitude in strain rate.

At both temperatures the constant load data can be represented with a very low scatter by the Monkman–Grant relationship which links the minimum strain rate to the rupture life. The Monkman–Grant exponent equals approximately −1, indicating that the same

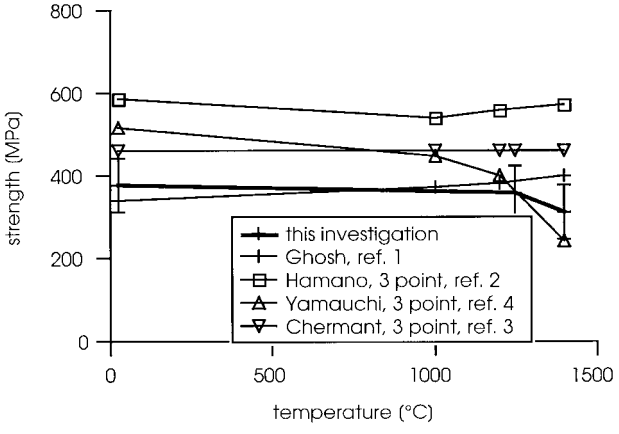

Fig. 1. Temperature dependence of average flexural strength.

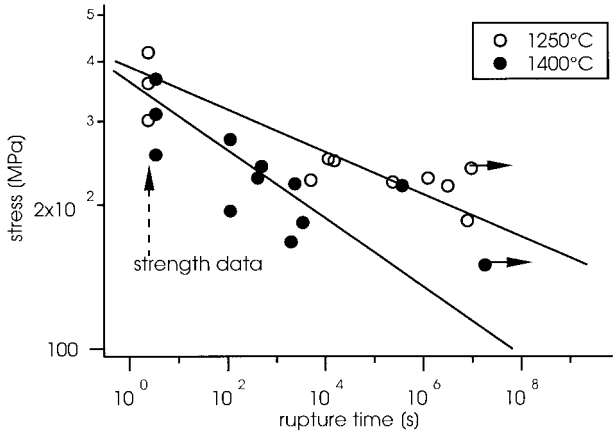

Fig. 2. Rupture lives as a function of applied flexural stress.

mechanism controls deformation and failure in the investigated stress-temperature range. Contrary to the stress dependencies of rupture time and minimum strain rate, however, the data from the strength tests do not fit the constant load regression line. When instead of the minimum strain rate the ratio of failure strain to failure time is used, the constant load and strength data at both temperatures can be represented by the same regression line and with very low scatter, as shown in Fig. 3. The exponent in this so-called Dobes–Milicka plot equals −1, indicating that failure of the material under all the investigated conditions (short term monotonic and long term constant load) is strain controlled. From the fit regression line in Fig. 3 an average strain to failure of (9.2±1.2) E-4 is obtained.

The large scatter in rupture time and the rather high stress exponents, together with the low failure strains and the fact that the scatter can be practically eliminated by the Dobes–Milicka approach, all suggest that failure under constant load conditions in the investigated stress-temperature range is controlled by subcritical crack growth (SCG) from pre-existing defects.

Combining Weibull strength statistics with the subcritical crack growth law derived from the constant load data allows to calculate the probability for a given lifetime at a given stress. This approach can be used to quantify the expected scatter in lifetime. The result at both temperatures is shown in Fig. 4 where the lines corresponding to failure probabilities of 5 and 95% are shown together with the experimental data. It can be observed that the short-life data are bound by the 5% probability line at both temperatures. This is not the case for one long-life experimental result at 1250°C, and two results at 1400°C. At the corresponding stress levels the failure probability is higher than 95%. In view of the relatively small number of specimens tested it is not reasonable to assume that this probability level is attained in the experiments. These three results at low applied stress therefore suggest the existence of a threshold stress below which failure by subcritical crack growth does not occur.

A threshold behaviour for SCG has been observed for a number of silicon carbide materials [5,6] and has been attributed to crack or flaw blunting by either the effect of oxidation or by the presence of cavitation ahead of the crack tip. In both cases the severity of the flaw is reduced to a level below which it can not grow. A recently developed model [7] for the growth of crack-like cavities between elastic grains describes the SCG behaviour in the presence of a threshold by the following equation:

$$v = \alpha[K/K_{th} + [(K/K_{th})^2 - 1]^{0.5}]^{12} \quad (1)$$

where v is the crack growth rate, K the applied stress intensity factor, K_{th} is the threshold stress intensity factor and α is a constant. The latter two parameters can be determined from fitting the equation to the experimental results presented in Fig. 1, as shown in Fig. 5. The value of the threshold intensity factor at both temperatures can be translated into a threshold stress of 215 MPa at 1250°C and 150 MPa at 1400°C.

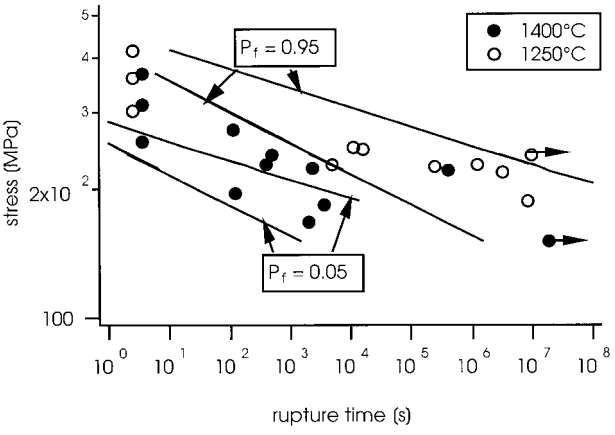

Fig. 4. Experimental rupture lives and failure probability lines.

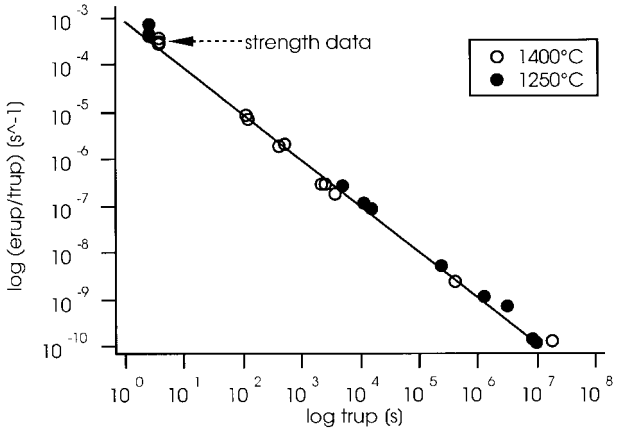

Fig. 3. Dobes–Milicka plot of constant load flexural data.

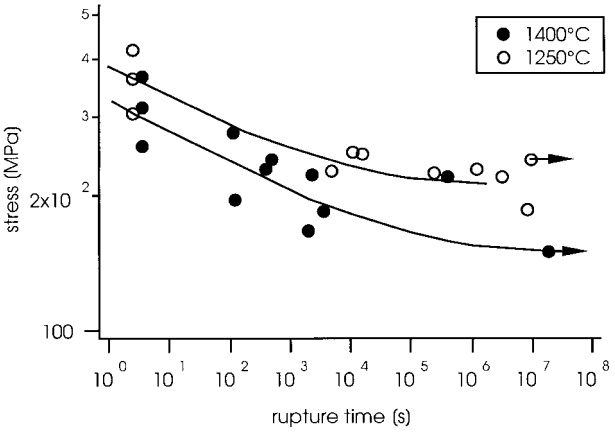

Fig. 5. Experimental failure times versus applied stress and best fits according to Chuang's model.

5. Long term uniaxial properties

Similarly to the flexure constant load tests, the strain versus time curves of the uniaxial constant load tests performed at 1400°C do not present a tertiary stage, but consist of a primary and a secondary part. A comparison of the strain accumulation between flexural and uniaxial load tests is shown in Fig. 6. Whereas in bend tests the strain continuously increases, this is not the case in the uniaxial tests at the lowest stresses. After load application, the strain remains approximately constant for a given time period and then increases to considerably higher levels. This suggests that an incubation time is required before the strain accumulates again. This period corresponds to the time required for the generation of a new flaw population which becomes dominant over the population of inherent flaws. A possible mechanism consists of healing of the inherent surface flaws by oxidation. Indeed, as indicated earlier at low applied stress levels SCG is overtaken by a blunting effect, resulting in threshold behaviour. Below the threshold another mechanism which is not related to SCG determines strain accumulation and ultimately lifetime. Such a time-dependent mechanism is true creep. The strain increase observed in uniaxial constant load tests after the incubation period can therefore be considered an indication of the transition from SCG to pure creep.

The uniaxial failure times are shown in Fig. 7, together with those calculated from the flexural constant load tests taking into account the Weibull size effect on strength according to the equation

$$t_f/t_t = (\sigma_{at}/\sigma_{af})^N (A_{eff,t}/A_{eff,f})^{(N-2)/m} \quad (2)$$

where subscripts t and f stand for tensile and flexure, respectively, A is the effective surface area, N is the SCG stress exponent, and m the Weibull modulus. Taking the scatter on the flexural constant load data into account, the uniaxial results agree with those obtained under flexural loading. The same applies for the minimum strain rate data. The good agreement evidences that for comparable applied stresses the rupture time in the uniaxial constant load tests is also governed by SCG.

The failure strains observed in both types of test at 1400°C are shown in Fig. 8. Below an applied stress of about 160 MPa and independent of loading mode, the strain to failure suddenly increases. This sharp transition corresponds within experimental error with the value of the threshold stress determined from the flexural constant load data. For higher applied stresses SCG prevails at 1400°C, whereas creep behaviour characterised by a larger strain accumulation dominates at lower stresses.

The Monkman–Grant plot of all the constant load data at 1400°C is shown in Fig. 9, where uniaxial data from literature [8] on a similar material in the temperature range from 1150 to 1350°C are included. These results agree remarkably well with the data from this investigation and confirm the temperature independence of the Monkman–Grant relationship. It is worthwhile to note that the experimental results for both the SCG

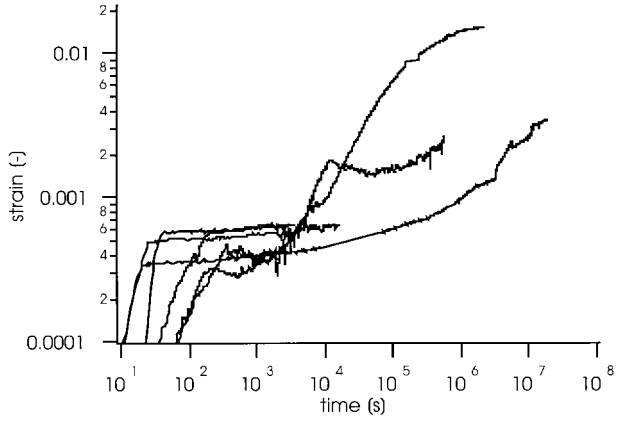

Fig. 6. Strain accumulation under constant load flexural tests (dashed) and uniaxial (solid lines) at 1400°C in the stress range from 150 to 183 MPa.

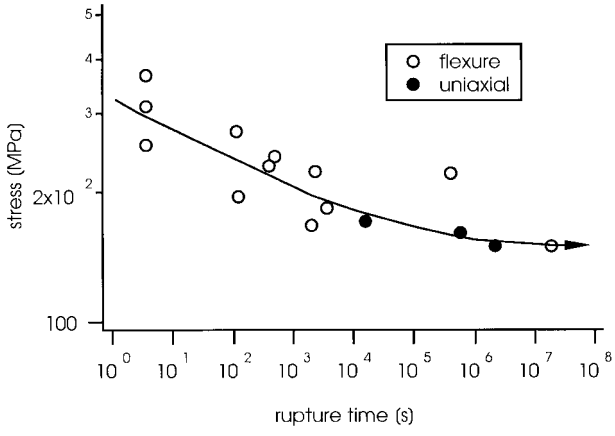

Fig. 7. Comparison of rupture times under uniaxial and flexural loading at the same nominal stresses at 1400°C.

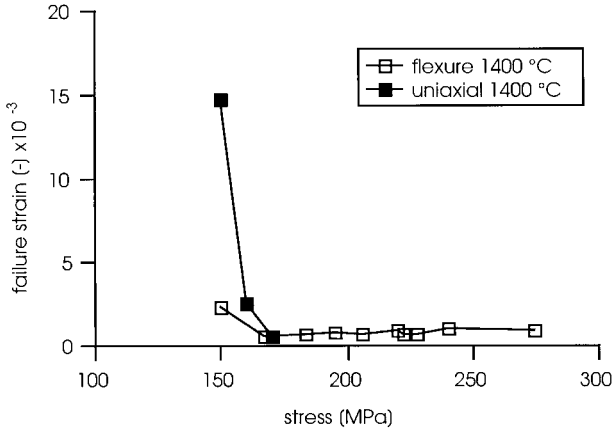

Fig. 8. Failure strains in uniaxial and flexural tests.

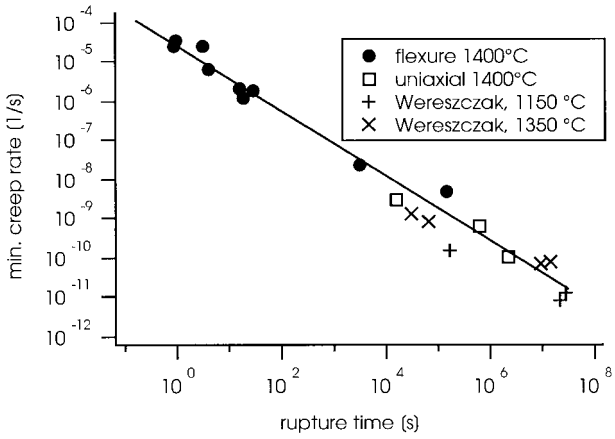

Fig. 9. Monkman–Grant plot of the flexure and uniaxial constant load data at 1400°C, and data from Ref. [8] at temperatures of 1150 and 1350°C.

and creep dominated regime fit the Monkman–Grant regression line, notwithstanding the fact that the failure strains in the tests exhibiting creep behaviour are considerably larger than for those where SCG prevails. The literature data at 1350°C experimentally span the SCG and creep dominated range and the minimum creep rate data clearly indicate that creep is diffusion controlled with a stress exponent equal to 1. It can hence be safely assumed that also for the investigated silicon carbide diffusion creep prevails below the threshold stress at any given temperature.

6. Discussion

It has been shown that the silicon carbide investigated here is susceptible to SCG at both temperatures of 1250 and 1400°C. This is somewhat surprising in view of the absence of an amorphous grain boundary phase which is usually considered to cause the sensitivity to SCG [9]. When no amorphous grain boundaries are present, SCG initiates at surface locations such as surface-connected porosity or machining flaws [10]. Also amorphous phases may form upon exposure to an oxidative environment (such as air), thereby triggering SCG. These observations indicate that the environment plays a major role in determining the time-dependent behaviour of the investigated sintered silicon carbide. This is also confirmed by other investigators who have shown that the sensitivity to SCG of sintered silicon carbides critically depends on the oxygen content of the environment [11]. It is hence to be expected that the values of the threshold stress for SCG obtained in this investigation are affected by the surface finish and by the environment.

The sensitivity to the surface finish is obviously more pronounced for specimens with a high surface to volume ratio, i.e. the bend specimens. Hence, typical features for SCG such as large scatter at a given stress in constant load tests, caused by a variability in the initial defect size from specimen to specimen, show up more clearly in the flexure tests. Conversely, the pure creep behaviour typical at low stresses, is expected to manifest itself more in uniaxial tests.

The good agreement between the results of constant load tests in the two loading modes is atypical for monolithic ceramics. The first reason lies in the fact that under the investigated stress- temperature conditions life is mostly dominated by SCG. However, for ceramics without amorphous intergranular phases the asymmetrical creep behaviour between tension and compression (as applies in flexure tests) is usually not apparent, and tensile and compressive creep are equal [12]. Hence, for such ceramics also under creep conditions a difference between flexural and uniaxial loading is not expected. This is further confirmed by the fact that the threshold stress marking the transition from SCG to creep behaviour does not depend on the loading mode.

For life prediction purposes the Larson–Miller parameter P_{LM} is often used. Applying regression analysis to the flexural data at both temperatures results in the following equations which describe the SCG-controlled regime of time-dependent mechanical behaviour:

$$P_{\mathrm{LM}} = T(C + \log t) \tag{3a}$$

$$\sigma = 679.2 - 14.618E - 3P_{LM} \qquad (\mathrm{MPa, s, K}) \tag{3b}$$

where T is temperature, t is time, σ is the applied stress and the constant C has been determined by minimising the experimental scatter. These equations apply for stresses above the threshold stress at temperature. For lower stresses diffusion creep failure occurs. The failure mechanism map shown in Fig. 10 summarises the failure mechanisms for the investigated silicon carbide. The map applies for specimens with an effective surface of 1000 mm^2 (corresponding to the size of the uniaxial test specimens) and delineates the regions where fast fracture, SCG and creep are life-limiting. The cross symbols on the vertical lines at 1250 and 1400°C represent fast fracture probabilities of 1, 5, 50, 95 and 99%. For the

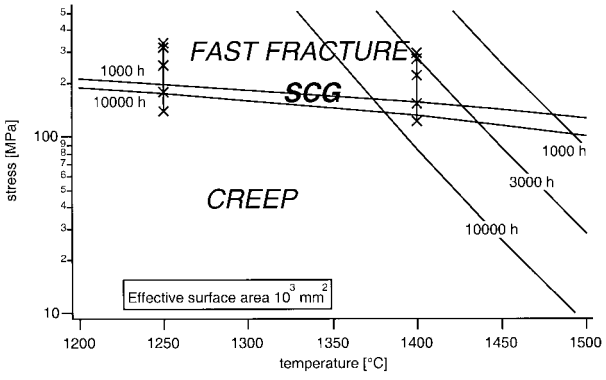

Fig. 10. Failure mechanism map for test pieces of the investigated silicon carbide with an effective surface area of 1000 mm^2.

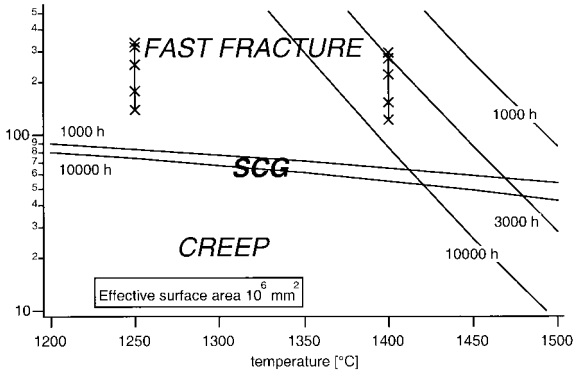

Fig. 11. Failure mechanism map based on an effective surface area of 10^6 mm^2.

SCG regime, two parameter lines with average lifetimes of 1000 and 10,000 h are shown. These lines fall within the low fast fracture probability range, as do the experimentally obtained threshold stresses of 215 MPa at 1250°C and 150 MPa at 1400°C. Also shown in the Figure are three parameter lines corresponding to predicted average failure times of 1000, 3000 and 10,000 h under creep conditions. Their intersection with the corresponding SCG parameter lines indicates that the transition stress hardly depends on temperature. In the creep dominated stress–temperature range the rupture life is orders of magnitude shorter than that predicted on the basis of an extrapolation of the SCG behaviour.

The failure mechanism map of Fig. 10 applies for test pieces with an effective surface area of 1000 mm^2. For components with a larger surface area and with the same surface finish as considered here, the stress values in the fast fracture and SCG region of the failure mechanism map scale according to Eq. (2). For an effective surface area of 1E6 mm^2, the stresses resulting in equal failure times for the same failure probability have to be rated down by a factor 0.42. The stresses and failure times corresponding to the creep regime are not affected by this size increase because they correspond to failure from a new flaw population generated during loading. The resulting failure mechanism map is shown in Fig. 11 where it can be seen that the overlap between the SCG and fast fracture regime increases, and that the occurrence of creep failure is suppressed to approximately below 55 MPa.

From the above figures it appears that accelerated constant load testing for life prediction purposes should preferably be performed below the transition stress between SCG and creep dominated behaviour. This implies that the acceleration should be realised by increasing temperature. Because the Monkman–Grant relationship does not depend on temperature, the accelerated constant load tests need not be continued to rupture but can be stopped after the minimum strain rate has been reached.

Acknowledgements

The authors would like to thank ENEL for granting IAM the authorisation to publish part of the results obtained within contract 2RTRI0015.

References

[1] A. Ghosh, M. Jenkins, K. White, A. Kobayashi, R. Bradt, J. Am. Ceram. Soc. 72 (1989) 242.
[2] Y. Hamano, M. Yamaguchi, S. Nagano, Sintered silicon carbide, in: E. Lenoe, R. Katz, J. Burke (Eds.), Ceramics for High-Performance Applications III, Reliability, Plenum Press, 1983, p. 251.
[3] J.L. Chermant, R. Moussa, F. Osterstock, Revue Internationale Hautes Températures et Réfractaires 18 (1981) 5.
[4] Y. Yamauchi, S. Sakai, M. Ito, T. Ohji, W. Kanematsu, S. Ito, J. Ceram. Soc. Jpn. 98 (1990) 250.
[5] K. McHenry, R. Tressler, Am. J. Ceram. Soc. 63 (1980) 152.
[6] E. Minford, J. Costello, I. Tsong, R. Tressler, Oxidation effects on crack growth and blunting in SiC ceramics, in: Fracture Mechanics of Ceramics, Vol. 6, 1983, p. 511
[7] T. Chuang, Am. J. Ceram. Soc. 65 (1982) 93.
[8] A. Wereszczak, T. Kirkland, Creep performance of candidate SiC and Si_3N_4 materials for land-based gas turbine engine components, ASME Turbo Expo '96 Conference, Birmingham, UK.
[9] G. Quinn, Static fatigue in high-performance ceramics, in: ASTM STP 844, 1984.
[10] R. Govila, J. Mater. Sci. 18 (1983) 1967.
[11] G. Campbell, B. Dalgleish, A. Evans, J. Am. Ceram. Soc. 72 (1989) 1402.
[12] S. Wiederhorn, B. Fields, B. Hockey, Mater. Sci. Eng. A176 (1994) 51.